

USE OF THE SURFACE HARMONICS METHOD FOR CALCULATION OF 2D BENCHMARK C5G7 MOX

Victor F. Boyarinov

Russian Research Center “Kurchatov Institute”, Nuclear Reactor Institute

123182, Moscow, RUSSIA

Boyarinov@dhtp.kiae.ru

ABSTRACT

Benchmark C5G7 MOX was proposed specially to test the ability of current transport codes to compute reactor core without use the procedure of spatial homogenization. Seven group cross sections for all materials were given. Just that fact allows to test an accuracy of solving neutron transport equation by different codes excluding additional errors connected with preparing group cross sections. In this paper, Surface Harmonics Method (SHM) is applied to compute the two-dimensional configuration of this benchmark. Different approximations of SHM were applied both without use procedure of spatial homogenization and with use this procedure. This fact allowed additionally carry out evaluation of the effect of spatial homogenization of cells. Comparisons were carried out for k_{eff} and pin powers with both the reference results and between the results calculated by different approximations of SHM. Besides, values of k_{∞} both for fuel pin cells and for fuel assemblies are presented.

1. INTRODUCTION

Expert Group on 3-D Radiation Transport Benchmarks proposed seven-group form of the C5 MOX problem [1] to test the ability of current transport codes to compute reactor core problems without use the procedure of spatial homogenization. Seven group cross sections for UO_2 , the three enrichments of MOX, the guide tubes, the fission chamber and the moderator were given. Just that fact allows to test an accuracy of solving neutron transport equation by different codes excluding additional errors connected with preparing group cross sections. Expert Group proposed to use the results calculated by Dr. M. Smith (ANL, USA) as a reference ones.

In this paper, Surface Harmonics Method [2] is applied to compute the two-dimensional configuration of this benchmark. SHM is the method for the solving neutron transport equation in a reactor core. A characteristic feature of SHM is that, in general case, it does not use the procedure of spatial homogenization, but if the homogeneous cross sections are used as initial information SHM works as a nodal method and solves diffusion equation. In SHM, neutron distribution in a reactor core is presented as a superposition of trial functions. Each trial function is taken as a solution of the neutron transport equation in the internal cell area with certain boundary conditions on the cell surface. Different trial functions differ from one another by the boundary conditions. Since the actual number of the trial functions is limited,

at substituting the quest solution in the neutron transport equation, a residual appears. The minimization procedure for this residual gives the finite-difference equations of the SHM. The main limitation of SHM is connected with the real number of used trial functions. For computation of trial functions, WIMS-SH [3] system of codes is used. WIMS-SH is alone code containing computational modules for solving group neutron transport equation in heterogeneous reactor cells with required boundary conditions. Now WIMS-SH can calculate only three first spatial trial functions for heterogeneous cells. For calculation of higher trial functions the procedure of spatial homogenization and diffusion approximation are used, in so doing SUHAM-2D [4] code is applied for solving group diffusion equation. Thus, the most accurate approximation of SHM without use the procedure of spatial homogenization is '3f(het)'. Approximation '3f(het)' means that three trial functions are used in so doing for calculation of these trial functions group neutron transport equation is solved in heterogeneous cells. Other approximations of SHM are forced to use the procedure of spatial homogenization and diffusion approximation for calculation of separate trial functions.

Concrete calculations were carried out by different approximations of SHM. The most accurate calculation was carried out with use of eight trial functions for each cell, in so doing the first three trial functions were calculated for heterogeneous cells and next five – for homogeneous cells (symbolic name '3f(het)+5f(hom)'). Comparisons of calculational results were carried out for k_{eff} and pin powers both between different approximations of SHM and with the reference solution calculated by Monte-Karlo method.

2. BRIEF DESCRIPTION OF SURFACE HARMONICS METHOD

In SHM, group function of neutron distribution in a reactor core is presented as a superposition of group trial matrices

$$\vec{\Phi}^N(w) = \sum_{i=1}^I \sum_{n=0}^N \hat{\phi}_i^{(n)}(w) \vec{I}_{in} \quad (1)$$

Here $\hat{\phi}_i^{(n)}(w)$ are the trial matrices describing the neutron field in i-th cell, vectors \vec{I}_{in} are the unknown group amplitudes, n - trial matrix number, (N+1) – total number of trial matrices for each cell, $w = \{\vec{r}, \vec{\Omega}\}$.

Each vector $\vec{\phi}_{ig}^{(n)}(w)$ of each trial matrix $\hat{\phi}_i^{(n)}(w)$ is taken as a solution of the group neutron transport equation in the internal cell area with certain boundary condition on the cell surface. For calculation of the vector $\vec{\phi}_{ig}^{(n)}(w)$ ($g=1,2,\dots,G$) the following boundary condition is used: incoming current for group 'g' is distributed on the external boundary as function of coordinates $W_k(\vec{r}_s)$ and for each another group this current equals zero for all points of external boundary. Functions $W_k(\vec{r}_s)$ are presented as follows

$$W_k(\vec{r}_s) = P_p(\rho_j) \begin{Bmatrix} \cos(l\alpha_j) \\ \sin(l\alpha_j) \end{Bmatrix}, \quad (2)$$

where

$$\begin{cases} \rho_j = (-1)^{j-1} \frac{2}{a} [\bar{r}_s - \frac{a}{2}(2j-1)], -1 \leq \rho_j \leq 1, 0 \leq r_s \leq Ma \\ \alpha_j = \frac{2\pi}{M}(j-1) \end{cases} \quad (3)$$

Here $P_p(\rho_j)$ – Legendre polynomials; M – number of lateral sides of cell; a – length of lateral side of cell; j - lateral side number of cell; α_j – angle between normal built from center of cell on j -th lateral side of cell and axis X . The lateral sides of cell are numbered against of a clock hand; the first lateral side of cell is the right side.

For cell with square external boundary, the first eight functions $W(\bar{r}_s)$ have the following forms

$$\begin{cases} W_0(\bar{r}_s) = 1, \quad W_1(\bar{r}_s) = \cos(\alpha_j), \quad W_2(\bar{r}_s) = \sin(\alpha_j) \\ W_3(\bar{r}_s) = \cos(2\alpha_j), \quad W_4(\bar{r}_s) = P_1(\rho_j), \quad W_5(\bar{r}_s) = P_1(\rho_j)\cos(\alpha_j), \\ W_6(\bar{r}_s) = P_1(\rho_j)\sin(\alpha_j), \quad W_7(\bar{r}_s) = P_1(\rho_j)\cos(2\alpha_j) \end{cases} \quad (4)$$

Since the actual number of the trial matrices is limited, at substituting the quest solution in the group neutron transport equation, a residual appears. The minimization procedure for this residual gives the finite-difference equations of the SHM. Finite-difference equations of SHM for square lattice with eight trial functions have the following form

$$\begin{cases} \hat{\Lambda}_0 \bar{\Phi}_k - \hat{\Sigma}_k \bar{\Phi}_k + \bar{S}_k^{(0)} = 0 \\ \hat{\Lambda}_0 \bar{X}_k^{(1)} + \hat{\Sigma}_k^{(1)} \bar{X}_k^{(1)} + \bar{S}_k^{(1)} = 0 \\ \hat{\Lambda}_2 \bar{X}_k^{(7)} + \hat{\Sigma}_k^{(2)} \bar{X}_k^{(2)} + \bar{S}_k^{(2)} = 0 \\ \hat{\Lambda}_3 \bar{X}_k^{(6)} + \hat{\Sigma}_k^{(3)} \bar{X}_k^{(3)} + \bar{S}_k^{(3)} = 0 \\ \hat{\Lambda}_0 \bar{X}_k^{(4)} + \hat{\Sigma}_k^{(4)} \bar{X}_k^{(4)} + \bar{S}_k^{(4)} = 0 \\ \hat{\Lambda}_0 \bar{X}_k^{(5)} + \hat{\Sigma}_k^{(5)} \bar{X}_k^{(5)} + \bar{S}_k^{(5)} = 0 \\ \hat{\Lambda}_2 \bar{X}_k^{(3)} - \hat{\Sigma}_k^{(6)} \bar{X}_k^{(6)} + \bar{S}_k^{(6)} = 0 \\ \hat{\Lambda}_3 \bar{X}_k^{(2)} - \hat{\Sigma}_k^{(7)} \bar{X}_k^{(7)} + \bar{S}_k^{(7)} = 0 \end{cases}, \text{ where } \begin{cases} \bar{S}_k^{(0)} = -\hat{\Lambda}'_1 \bar{X}_k^{(1)} - \hat{\Lambda}'_3 \bar{X}_k^{(6)} - \hat{\Lambda}'_2 \bar{X}_k^{(7)} \\ \bar{S}_k^{(1)} = -\hat{\Lambda}'_1 \bar{\Phi}_k - \hat{\Lambda}'_3 \bar{X}_k^{(6)} + \hat{\Lambda}'_2 \bar{X}_k^{(7)} \\ \bar{S}_k^{(2)} = -\hat{\Lambda}'_6 (\bar{\Phi}_k - \bar{X}_k^{(1)}) \\ \bar{S}_k^{(3)} = -\hat{\Lambda}'_7 (\bar{\Phi}_k + \bar{X}_k^{(1)}) \\ \bar{S}_k^{(4)} = \hat{\Lambda}'_1 \bar{X}_k^{(5)} - \hat{\Lambda}'_3 \bar{X}_k^{(2)} - \hat{\Lambda}'_2 \bar{X}_k^{(3)} \\ \bar{S}_k^{(5)} = \hat{\Lambda}'_1 \bar{X}_k^{(4)} - \hat{\Lambda}'_3 \bar{X}_k^{(2)} + \hat{\Lambda}'_2 \bar{X}_k^{(3)} \\ \bar{S}_k^{(6)} = -\hat{\Lambda}'_6 (\bar{X}_k^{(4)} - \bar{X}_k^{(5)}) \\ \bar{S}_k^{(7)} = -\hat{\Lambda}'_7 (\bar{X}_k^{(4)} + \bar{X}_k^{(5)}) \end{cases} \quad (5)$$

Here $\hat{\Lambda}_i, \hat{\Lambda}'_i$ - different types of finite-difference operator, $\bar{\Phi}_k, \bar{X}_k^{(l)}$ - unknown vectors connected with the different laws of neutron incoming. Coefficients $\hat{\Sigma}_k^{(i)}, \hat{D}_k^{(j)}$ are functionals of trial matrices in so doing coefficients $\hat{D}_k^{(j)}$ ($j=1,2$) are hid in finite-difference operators.

Finite-difference equations of SHM with four trial functions have the following form

$$\begin{cases} \hat{\Lambda}_0 \bar{\Phi}_k - \hat{\Sigma}_k \bar{\Phi}_k + \bar{S}_k^{(0)} = 0 \\ \hat{\Lambda}_0 \bar{X}_k^{(1)} + \hat{\Sigma}_k^{(1)} \bar{X}_k^{(1)} + \bar{S}_k^{(1)} = 0 \end{cases}, \quad (6)$$

Finite-difference equations in the lowest approximation of SHM with three trial functions have the following form

$$\hat{\Lambda}_0 \bar{\Phi}_k - \hat{\Sigma}_k \bar{\Phi}_k = 0, \quad (7)$$

It should be noted, that all SHM characteristics $\hat{\Sigma}_k^{(i)}$, $\hat{D}_k^{(j)}$ depend on the unknown value of k_{eff} and so an additional iteration layer is organized.

3. USED CODES

WIMS-SH system of codes and SUHAM-2D code were used for computation of this benchmark. WIMS-SH is alone code containing computational modules for solving group neutron transport equation in heterogeneous reactor cell with required boundary conditions. Now WIMS-SH can calculate only three first spatial trial matrices for heterogeneous cells. For calculation of elements of the zeroth trial matrix $\hat{\phi}^{(0)}$ RATIA option [3] of WIMS-SH code is used. In RATIA code, G_3 approximation of Surface Pseudo Sources Method is used for solving the group neutron transport equation. In this method, surface Green function is used in every homogeneous zone of cell. Concerning angular variable G_3 approximation corresponds P_3 approximation. For calculation of the first and the second trial matrices for cells $\hat{\phi}^{(1)}$, $\hat{\phi}^{(2)}$ new option DIC-PN of WIMS-SH code was used. In DIC-PN code, P_2 approximation of Spherical Harmonics method is used.

Procedure of spatial homogenization was used for calculation of the higher trial matrices from $\hat{\phi}^{(3)}$ up to $\hat{\phi}^{(7)}$. In so doing WIMS-SH code was used for preparation of homogeneous group cross sections for cells and SUHAM-2D code was used for solving group diffusion equation in cells with corresponding boundary conditions and in this case the cell was divided in 100 square meshes (10×10). For methodical purposes procedure of spatial homogenization and diffusion approximation were also used for calculation of the first three trial matrices.

Designate concrete calculations by symbolic name 'nf(het)+mf(hom)'. This designation means that n first trial matrices ($0 \leq n \leq 3$) are calculated by WIMS-SH system of codes, in so doing the group neutron transport equation is solved and m next trial matrices ($0 \leq m \leq 8$) are calculated by SUHAM-2D code, in so doing procedure of spatial homogenization is used and diffusion equation is solved.

4. DESCRIPTION OF CALCULATIONAL BENCHMARK.

Expert Group on 3-D Radiation Transport Benchmarks proposed C5G7 MOX benchmark to test the ability of current transport codes to compute reactor core without use the procedure of spatial homogenization. The quarter of two-dimensional configuration shown in Figure 1 consists of two MOX and two UO₂ assemblies and reflector. Overall dimensions of this configuration part are 64.26×64.26 cm while dimensions of each assembly are 21.42×21.42 cm.

Each fuel assembly is made up of a 17×17 lattice of square pin cells, as seen in Figure 2. All cells - fuel-pin cell, cell with guide tube and cell with fission chamber - consist of two zones, in so doing, for example, the internal material of fuel-pin cell is the material in which fuel, gap and cladding are homogenized and there is no fuel-coolant homogenization. The side length of every cell is 1.26 cm, the radius of every internal rod cylinder is 0.54 cm. There were four types of fuel in rods, namely, one type of UO₂ fuel and three types of MOX fuel with enrichment 4.3 %, 7.0 % and 8.7 %. A single moderator material is provided for use in all cells and in external moderator. Benchmark composition for four fuel assemblies and numbering scheme are shown in Figure 2.

Seven group cross-sections were given for following seven materials: four types of fuel materials, material of fission chamber, material of guide tube and material of moderator. Scattering cross-sections with transport correction were used.

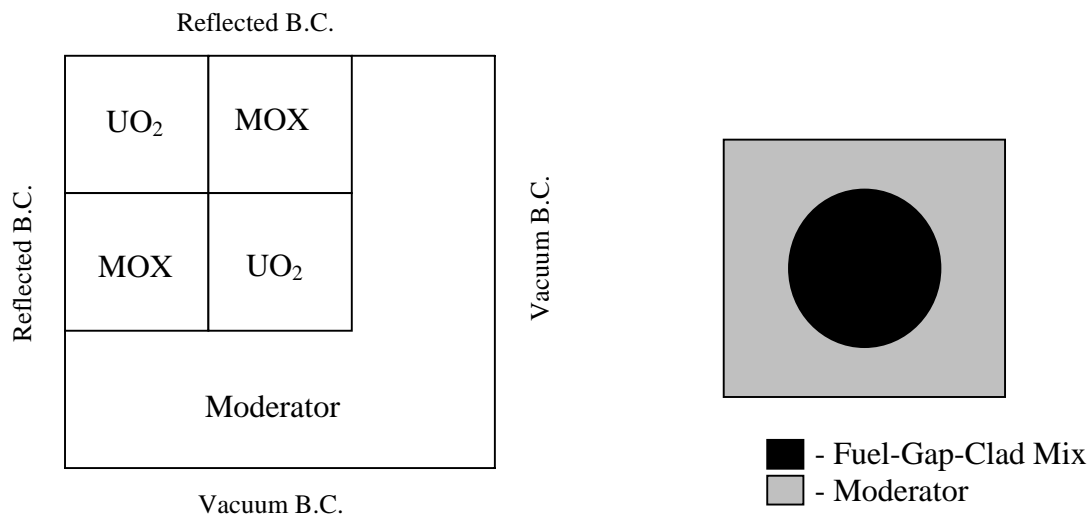


Figure 1. Two-dimensional configuration for C5G7 benchmark and fuel pin layout.

5. PERFORMED CALCULATIONS AND RESULTS.

Values of k_{∞} for four types of fuel-pin cells, calculated by RATIA option of WIMS-SH system of codes are presented in Table I.

Table I. Values of k_{∞} for fuel-pin cells

Fuel in rod	UO ₂	MOX, 4.3%	MOX, 7.0%	MOX, 8.7%
Value				
k_{∞}	1.32727	1.13591	1.15962	1.17245

Values of k_{∞} for two types of fuel assemblies, calculated by WIMS-SH and SUHAM-2D codes by different approximations of SHM are presented in Table II.

Table II. Values of k_{∞} for two types of fuel assemblies

Fuel	UO ₂	MOX
Approx.		
3f(hom)	1.33571 (-1)*	1.18389 (-8)
4f(hom)	1.33622 (37)	1.18404 (4)
8f(hom)	1.33634 (46)	1.18407 (7)
1f(het)+2f(hom)	1.33510 (-47)	1.18382 (-14)
1f(het)+3f(hom)	1.33561 (-9)	1.18399 (0)
1f(het)+7f(hom)	1.33574 (1)	1.18404 (4)
3f(het)	1.33509 (-48)	1.18374 (-21)
3f(het)+1f(hom)	1.33561 (-9)	1.18395 (-3)
3f(het)+5f(hom)	1.33573	1.18399

*) In brackets deviation from value in approximation '3f(het)+5f(hom)' is given.

Values of k_{eff} for considered 2D benchmark, calculated by WIMS-SH and SUHAM-2D codes by different approximations of SHM are presented in Table III. Beside, total CPU time in Pentium4-1500MHz for all calculations are presented in Table III

Table III. Values of k_{eff} for considered 2D benchmark

Approximation	k_{eff}	δk_{eff} , pcm ^{*)}	Total CPU time
3f(hom)	1.18600	-46, -29	2 min 1 sec
4f(hom)	1.18641	-12, 6	6 min 37 sec
8f(hom)	1.18647	-7, 11	60 min 25 sec
1f(het)+2f(hom)	1.18598	-48, -30	3 min 22 sec
1f(het)+3f(hom)	1.18640	-13, 5	7 min 13 sec
1f(het)+7f(hom)	1.18646	-8, 10	43 min 32 sec
3f(het)	1.18584	-60, -42	3 min 10 sec
3f(het)+1f(hom)	1.18628	-23, -5	8 min 20 sec
3f(het)+5f(hom)	1.18634	-18, —	32 min 51 sec
Reference	1.18655	—	—

*) The first value is deviation from reference value; the second value is deviation from value in approximation '3f(het)+5f(hom)'.

One can see that both k_{∞} of fuel assemblies and k_{eff} of considered 2D benchmark depend on the used calculational procedure very weakly.

Distribution of pin powers for considered 2D benchmark with average pin power normalized to 1 fission/sec/cell and calculated by '3f(het)+5f(hom)' approximation is presented in Figure 3 and Table IV. It should be noted that in all calculations maximum of pin powers is placed in points $(n_y, n_x) = \{(4,5), (5,4)\}$, and minimum of pin powers is placed in point $(n_y, n_x) = (33,33)$. Percent deviations of pin powers in separated points calculated by different approximations of SHM from corresponding values in reference and '3f(het)+5f(hom)' calculations are presented in Table V and Table VI correspondingly.

In all calculations at solving the finite-difference equations the following relative accuracies of convergence were used: 10^{-6} for eigenvalue and 10^{-5} for group local fluxes. Besides, for k_{eff} in additional iteration layer relative accuracy 10^{-5} was used.

CONCLUSIONS.

Surface Harmonics Method was applied to compute the two-dimensional configuration of the C5G7 MOX benchmark. Different approximations of SHM were used both without use the procedure of spatial homogenization and with use this procedure for calculation both the separate trial matrices and all trial matrices. Comparisons of calculational results were carried out for k_{eff} and pin powers. Besides, values of k_{∞} for both separate fuel pin cells and separate fuel assemblies are presented.

Analysis of obtained results allows do the following conclusions.

- In all calculations, both for C5G7 MOX benchmark and for fuel assemblies the eigenvalues are very close to one another.
- In all calculations of C5G7 MOX benchmark the maximum of pin powers is placed in points $(n_y, n_x) = \{(4,5), (5,4)\}$, and minimum of pin powers is placed in point $(n_y, n_x) = (33,33)$.
- There is not gradual approaching the pin powers calculated by different approximations of SHM to reference results. At the same time, there is gradual approaching the pin powers calculated by different approximations of SHM to results calculated by the most accurate approximation of SHM, namely '3f(het)+5f(hom)'.
- Deviation of pin powers in the most accurate approximation of SHM '3f(het)+5f(hom)' from the reference pin power reaches 4.3% in so doing this deviation takes place on the boundary of the MOX assembly with reflector.
- Deviation of pin powers in the most accurate approximation without use the procedure of spatial homogenization '3f(het)' from pin powers in the '3f(het)+5f(hom)' reaches 3.8%.
- Deviation of pin powers in '3f(het)+1f(hom)' calculation from pin powers in calculation '3f(het)+5f(hom)' reaches 0.7%. Calculation '3f(het)+1f(hom)' is the most preferable approximation of SHM on totality of two parameters, namely the accuracy and the time expenditure.
- Deviation of pin powers in the best possible approximation using the procedure of spatial homogenization '8f(hom)' from pin powers in calculation '3f(het)+5f(hom)' reaches 1.9%.
- Calculations with three trial matrices namely '3f(hom)', '1f(het)+2f(hom)' and '3f(het)' have not enough accuracy in pin powers - 3 and more percent from '3f(het)+5f(hom)'.
- The higher spatial harmonics (trial matrices from $\hat{\phi}^{(4)}$ up to $\hat{\phi}^{(7)}$) are not very essential for this benchmark, maximum deviation of pin powers in calculation '4f(hom)' from '8f(hom)' one, in calculation '1f(het)+3f(hom)' from '1f(het)+7f(hom)' one and in calculation '3f(het)+1f(hom)' from '3f(het)+5f(hom)' one equals 0.7 - 0.8 %.

- If zeroth trial matrix $\hat{\phi}^{(0)}$ is calculated by WIMS-SH it is not very large difference to use or not the procedure of spatial homogenization for calculation the higher matrices $\hat{\phi}^{(n)}$ ($n \geq 1$): maximum deviation of pin powers in calculation '1f(het)+2f(hom)' from '3f(het)' one, in calculation '1f(het)+3f(hom)' from '3f(het)+1f(hom)' one and in calculation '1f(het)+7f(hom)' from '3f(het)+5f(hom)' one is not more than 0.5%.

REFERENCES

1. E.E. Lewis, et al. *Benchmark specification for Deterministic 2-D/3-D MOX fuel assembly transport calculations without spatial homogenization (C5G7 MOX)*, NEA/NSC/DOC(2001)17, Salt Lake City, USA (2001).
2. N.I. Laletin. "On the Equations of Heterogeneous Reactor", *Voprosi Atomnoi Nauki i Tehniki. Ser. Fizika Yadernih Reactorov*, **5**, **18**, pp. 31-46, (1981) (in Russia).
3. N.I. Laletin, N.V. Sultanov, V.F. Boyarinov, et al. "WIMS-SU complex of codes and SPEKTR code", *Proceeding. of 'PHYSOR-90'*, Marseilles, France, April 23-27, 1990, v.4, p. PV-148, ANS/ENS, (1990).
4. V.F. Boyarinov, "SUHAM-2.5 Code for Solving 2D Finite-Difference Equations of the Surface Harmonics Method in Square and Triangular Lattices", *Nuclear Technology'99*, Karlsruhe, Germany, May 18-20, 1999, pp. 23-26 (1999).

Table IV. Distribution of pin powers in approximation '3f(het)+5f(hom)'.

	1	2	3	4	5	6	7	8	9	10	11	12	13	14	15	16	17		
1	2.205	2.210	2.220	2.231	2.240	2.233	2.199	2.161	2.123	2.068	2.012	1.953	1.866	1.760	1.637	1.483	1.271		
2		2.223	2.249	2.282	2.330	2.373	2.281	2.239	2.248	2.144	2.086	2.074	1.943	1.802	1.660	1.492	1.271		
3			2.332	2.440	2.487		2.380	2.331		2.233	2.175		2.075	1.929	1.726	1.513	1.275		
4					2.519	2.449	2.324	2.274	2.288	2.178	2.125	2.139	2.098		1.810	1.538	1.282		
5						2.449	2.427	2.310	2.261	2.275	2.166	2.113	2.122	2.041	1.990	1.844	1.574	1.289	
6								2.345	2.298		2.203	2.145		2.028	1.934		1.607	1.288	
7									2.248	2.207	2.222	2.115	2.059	2.055	1.931	1.838	1.765	1.544	1.269
8										2.168	2.183	2.078	2.023	2.016	1.893	1.802	1.732	1.518	1.250
9																			
10																			
11																			
12																			
13																			
14																			
15																			
16																			
17																			

Continuation of Table IV.

	18	19	20	21	22	23	24	25	26	27	28	29	30	31	32	33	34						
18	0.783	0.779	0.761	0.740	0.717	0.688	0.651	0.613	0.576	0.536	0.496	0.459	0.419	0.383	0.363	0.384	0.513						
19		0.819	0.827	0.820	0.812	0.800	0.740	0.696	0.670	0.610	0.565	0.537	0.481	0.433	0.407	0.422	0.542						
20			0.866	0.893	0.887		0.793	0.745		0.655	0.607		0.530	0.479	0.436	0.437	0.549						
21					0.894	0.843	0.772	0.726	0.700	0.638	0.593	0.570	0.535		0.456	0.442	0.545						
22						0.850	0.818	0.753	0.709	0.684	0.624	0.581	0.557	0.513	0.487	0.457	0.443	0.535					
23								0.745	0.702		0.620	0.575		0.499	0.462		0.440	0.518					
24									0.691	0.653	0.633	0.578	0.537	0.512	0.462	0.427	0.416	0.412	0.496				
25										0.619	0.599	0.548	0.509	0.485	0.437	0.404	0.393	0.391	0.472				
26												0.532	0.494		0.425	0.392		0.379	0.447				
27													0.486	0.452	0.431	0.389	0.359	0.351	0.348	0.419			
28														0.421	0.401	0.363	0.336	0.327	0.324	0.391			
29																0.349	0.323		0.309	0.363			
30																		0.322	0.305	0.288	0.278	0.333	
31																				0.261	0.250	0.304	
32																					0.235	0.231	0.279
33																						0.228	0.269
34																							0.293

Continuation of Table IV.

	18	19	20	21	22	23	24	25	26	27	28	29	30	31	32	33	34
1	1.325	1.061	0.930	0.857	0.808	0.762	0.710	0.661	0.615	0.566	0.520	0.478	0.432	0.391	0.369	0.407	0.625
2	1.309	1.355	1.175	1.095	1.060	1.041	0.930	0.860	0.834	0.740	0.678	0.651	0.569	0.499	0.465	0.518	0.617
3	1.301	1.330	1.183	1.162	1.117		0.939	0.859		0.745	0.678		0.600	0.530	0.470	0.508	0.612
4	1.302	1.339	1.248		1.109	1.117	0.967	0.888	0.867	0.765	0.702	0.692	0.583		0.500	0.512	0.611
5	1.306	1.376	1.283	1.177	1.162	1.073	0.935	0.860	0.842	0.741	0.679	0.667	0.614	0.530	0.508	0.526	0.612
6	1.304	1.421		1.265	1.131		0.972	0.890		0.774	0.702		0.609	0.564		0.544	0.610
7	1.286	1.349	1.205	1.155	1.044	1.024	0.906	0.837	0.821	0.723	0.661	0.642	0.560	0.519	0.473	0.517	0.604
8	1.267	1.327	1.181	1.131	1.023	1.004	0.891	0.825	0.810	0.713	0.652	0.632	0.551	0.509	0.465	0.510	0.599
9	1.250	1.356		1.175	1.059		0.930	0.856		0.746	0.676		0.577	0.528		0.525	0.594
10	1.223	1.283	1.145	1.097	0.993	0.977	0.867	0.803	0.790	0.696	0.636	0.618	0.539	0.498	0.455	0.499	0.586
11	1.196	1.258	1.124	1.081	0.979	0.961	0.854	0.791	0.777	0.685	0.628	0.610	0.533	0.494	0.451	0.494	0.578
12	1.170	1.281		1.147	1.030		0.892	0.819		0.716	0.652		0.567	0.525		0.509	0.572
13	1.130	1.200	1.127	1.035	1.027	0.956	0.836	0.772	0.760	0.671	0.616	0.608	0.560	0.483	0.466	0.483	0.562
14	1.084	1.128	1.063		0.955	0.967	0.842	0.778	0.764	0.677	0.623	0.617	0.522		0.450	0.462	0.551
15	1.042	1.088	0.986	0.982	0.952		0.810	0.746		0.654	0.599		0.535	0.474	0.422	0.455	0.546
16	1.012	1.099	0.988	0.941	0.924	0.915	0.826	0.770	0.752	0.672	0.619	0.597	0.526	0.464	0.433	0.478	0.555
17	1.015	0.913	0.857	0.820	0.789	0.755	0.712	0.669	0.629	0.584	0.540	0.499	0.455	0.415	0.392	0.421	0.599

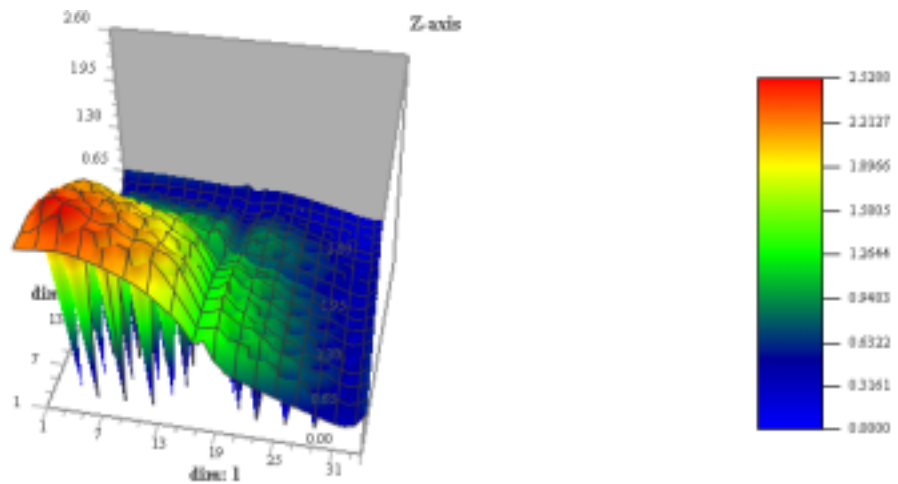


Figure 3. Pin powers distribution.

Table V. Percent deviations of pin power in separated points from reference

(ny,nx)	3f(hom)	4f(hom)	8f(hom)	1f(het)+ 2f(hom)	1f(het)+ 3f(hom)	1f(het)+ 7f(hom)	3f(het)	3f(het)+ 1f(hom)	3f(het)+ 5f(hom)
(1,1)	0.49	0.40	0.32	0.65	0.56	0.47	0.52	0.43	0.34
(1,9)	0.65	-0.00	0.16	0.76	0.13	0.28	0.64	-0.01	0.14
(1,17)	-0.63	-1.57	-1.60	-0.03	-0.94	-0.98	0.09	-0.83	-0.86
(1,18)	0.72	1.24	1.22	0.40	0.91	0.88	0.55	1.07	1.04
(1,26)	-0.48	-1.95	-1.68	-0.04	-1.46	-1.19	0.13	-1.36	-1.10
(1,34)	1.93	5.01	5.07	0.48	3.43	3.49	0.72	3.77	3.83
(9,10)	0.95	-0.11	0.06	0.87	-0.16	0.002	0.78	-0.27	-0.10
(9,17)	-0.37	-1.87	-1.66	0.21	-1.25	-1.05	0.35	-1.13	-0.93
(9,18)	0.56	0.35	0.55	0.40	0.19	0.38	0.60	0.35	0.54
(9,25)	-0.36	-2.26	-1.90	-0.41	-2.25	-1.90	-0.17	-2.16	-1.82
(9,34)	2.02	4.61	4.81	0.71	3.18	3.37	1.07	3.57	3.76
(17,17)	-1.62	-2.35	-2.53	-0.75	-1.46	-1.64	-0.56	-1.27	-1.45
(17,18)	0.10	0.16	0.22	-0.29	-0.22	-0.17	-0.12	-0.04	0.02
(17,26)	-0.36	-0.64	-0.42	-0.48	-0.75	-0.53	-0.25	-0.57	-0.36
(17,34)	1.79	5.20	5.28	0.05	3.32	3.38	0.30	3.60	3.67
(18,18)	-1.93	-2.45	-2.69	-1.01	-1.52	-1.75	-0.88	-1.37	-1.61
(18,26)	-1.65	-3.03	-2.86	-1.04	-2.38	-2.21	-0.84	-2.19	-2.02
(18,34)	0.64	2.91	2.85	-0.22	1.97	1.91	-0.12	2.14	2.08
(26,27)	-1.47	-2.25	-2.10	-1.59	-2.34	-2.19	-1.45	-2.21	-2.06
(26,34)	0.61	2.84	2.98	-0.57	1.56	1.70	-0.52	1.63	1.77
(34,34)	0.46	4.36	4.48	-1.42	2.30	2.41	-1.34	2.40	2.51
(4,5)	0.49	1.31	1.10	0.79	1.21	1.00	0.65	1.07	0.86
(33,33)	-2.00	-0.94	-0.96	-2.46	-1.36	-1.38	-2.38	-1.31	-1.33
Max. dev. and points	-3.87 (32,32)	5.42 (34,7), (7,34)	5.34 (5,34), (34,5)	-3.93 (32,32)	3.98 (7,34), (34,7)	3.90 (5,34), (34,5)	-3.79 (32,32)	4.38 (34,7), (7,34)	4.30, (5,34), (34,5)

Table VI. Percent deviations of pin power in separated points from '3f(het)+5f(hom)'

(ny,nx)	3f(hom)	4f(hom)	8f(hom)	1f(het)+ 2f(hom)	1f(het)+ 3f(hom)	1f(het)+ 7f(hom)	3f(het)	3f(het)+ 1f(hom)
(1,1)	0.15	0.06	-0.02	0.31	0.21	0.13	0.18	0.08
(1,9)	0.50	-0.15	0.02	0.62	-0.02	0.14	0.49	-0.16
(1,17)	0.24	-0.71	-0.74	0.84	-0.08	-0.12	0.96	0.03
(1,18)	-0.32	0.20	0.17	-0.63	-0.13	-0.16	-0.49	0.03
(1,26)	0.62	-0.86	-0.59	1.08	-0.36	-0.09	1.25	-0.26
(1,34)	-1.83	1.14	1.20	-3.23	-0.38	-0.33	-2.99	-0.05
(9,10)	1.05	-0.01	0.16	0.98	-0.05	0.11	0.88	-0.16
(9,17)	0.57	-0.94	-0.73	1.16	-0.32	-0.12	1.30	-0.20
(9,18)	0.03	-0.18	0.01	-0.14	-0.35	-0.16	0.06	-0.18
(9,25)	1.48	-0.45	-0.09	1.44	-0.44	-0.09	1.68	-0.35
(9,34)	-1.67	0.83	1.01	-2.93	-0.55	-0.37	-2.59	-0.18
(17,17)	-0.17	-0.91	-1.10	0.71	-0.01	-0.20	0.90	0.18
(17,18)	0.08	0.15	0.21	-0.30	-0.24	-0.18	-0.13	-0.06
(17,26)	0.01	-0.29	-0.07	-0.12	-0.40	-0.18	0.10	-0.22
(17,34)	-1.82	1.48	1.55	-3.49	-0.34	-0.28	-3.25	-0.06
(18,18)	-0.33	-0.85	-1.10	0.61	0.10	-0.14	0.74	0.24
(18,26)	0.38	0.38	-0.85	1.01	-0.36	-0.19	1.21	-0.17
(18,34)	-1.41	0.82	0.75	-2.25	-0.10	-0.16	-2.16	0.06
(26,27)	0.59	-0.20	-0.04	0.47	-0.29	-0.14	0.62	-0.16
(26,34)	-1.14	1.05	1.19	-2.30	-0.21	-0.07	-2.25	-0.14
(34,34)	-2.01	1.80	1.92	-3.83	-0.20	-0.10	-3.76	-0.10
(4,5)	0.01	0.45	0.23	-0.07	0.35	0.13	-0.21	0.21
(33,33)	-0.68	0.40	0.38	-1.14	-0.03	-0.05	-1.06	0.02
Max. dev. and points	-2.62 (30,5), (5,30)	1.80 (34,34)	1.92 (34,34)	-3.83 (34,34)	-0.704 (23,4), (4,23)	0.47 (15,33), (33,15)	-3.76 (34,34)	-0.73 (6,31), (31,6)

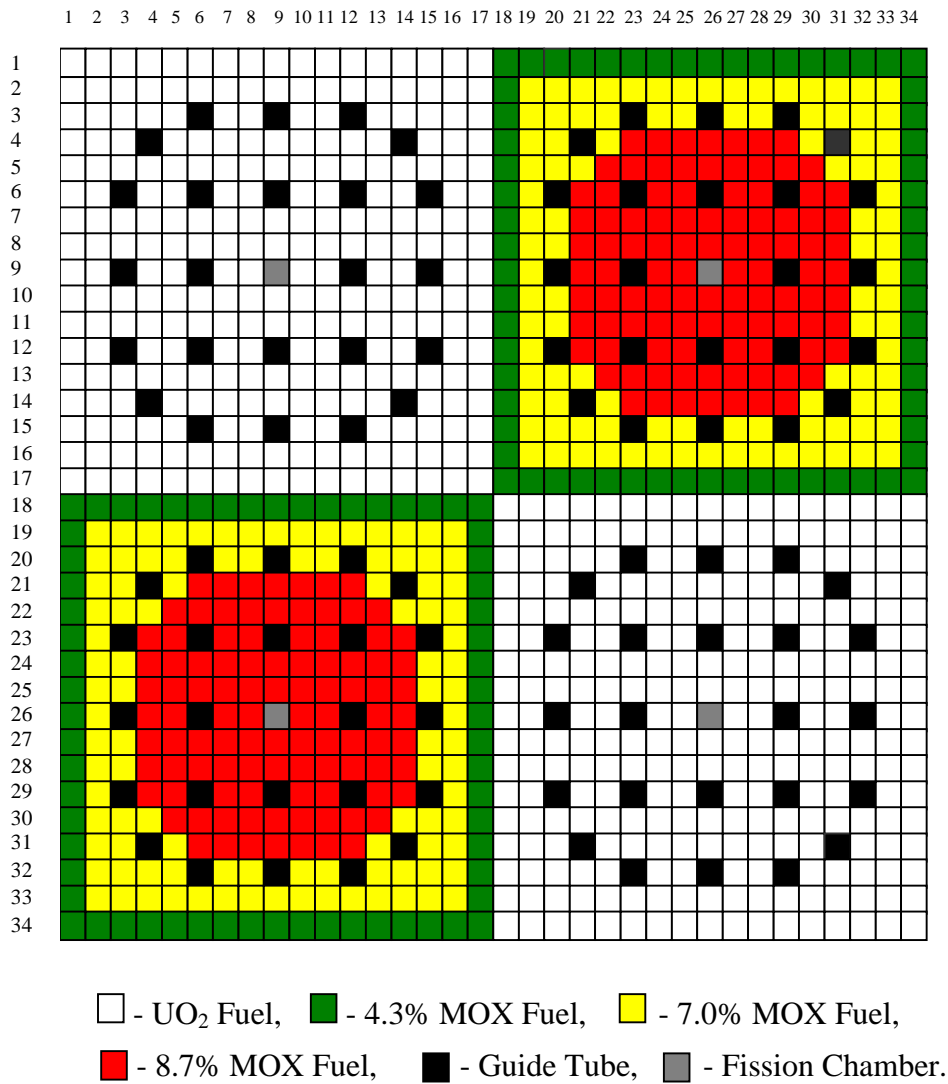


Figure 2. Benchmark composition for four fuel assemblies and numbering scheme.